European Science Methodical Journal
ISSN (E): 2938-3641
Volume 4, Issue 2, February - 2026

CHARACTERIZATION OF QUANTUM EFFICIENCY AND OPTICAL ABSORPTION OF NANOMATERIAL DRUG CARRIERS UNDER LASER EFFECT: THEORETICAL AND PRACTICAL INSIGHTS

Zainab A. Elzahra 1*,
Fatima Abbas Shaker1
1Department of Vision Screening Techniques,
College of Health and Medical Techniques,
Al-Furat Al-Awsat Technical University, An-Najaf, Iraq
* zainab.hassanchm@atu.edu.iq

Abstract:

To successfully combine laser technology with nanomedicine, it is important to have a good insight into the optical properties of drug carriers. The paper will describe the Quantum Efficiency (QE) and Optical Absorption of two different types of nanomaterials: carbon-based Graphene Quantum Dots (GQDs) synthesized by hydrothermal, biogenic (green), and Laser Ablation in Liquids (LAL) synthesis, and metallic nanoparticles (AgNPs and AuNPs). The main goal was to establish the correlation between structural property - e.g. particle size, surface defects and functionalization - and the photonic performance of the material under laser irradiation. It was shown in the experiment that LAL-produced AuNPs are more monodispersed and reach a high Surface Plasmon Resonance (SPR) peak at 520 nm as compared to other methods, which are more suited to photothermal work. On the other hand, organic capping layers resulted in broader absorption profiles in biogenic AgNPs. GQDs exhibited a high intrinsic QE of 18.4 percent with regards to the carbon-based carriers. When loaded with the anticancer drug Doxorubicin (DOX), the QE considerably dropped to 9.2% which is due to a Fluorescence Resonance Energy Transfer (FRET) process, essentially acting as an optical signal-off detector in drug conjugation. In order to triangulate these experimental results, DFT calculations were done with the B3LYP functional. The theoretical models estimated a decrease in HOMO-LUMO gap to 2.98 eV (GQD-DOX complex) compared to 3.65 eV (bare GQD) which was consistent with experimental optical data with a variation of less than 6%. As the current paper confirms, the combination of advanced laser spectroscopy and theoretical modeling allows building a powerful framework of the design of smart, optically active drug delivery system.

Keywords: Nanomaterial Characterization, Quantum Efficiency, Optical Absorption, Laser Ablation in Liquids, Graphene Quantum Dots, Density Functional Theory (DFT), Surface Plasmon Resonance, Drug Delivery Systems, Biogenic Synthesis, Dynamic Light Scattering (DLS).

Introduction

The application of nanotechnology in the field of biomedical sciences has completely changed the field of drug delivery and diagnostic imaging. The most fundamental aspect of this change is manipulation of matter at the atomic and molecular scale to design materials with desired optical, electronic and physical properties that are not found in bulk materials [1-2]. The mission in the particular case of drug delivery has been to turn the transportation into smart, responsive systems. They are meant to deliver therapeutic agents to specific sites and timings, in many cases, in response to external stimuli. One of these stimuli is light (or more precisely laser irradiation), which can be used as a primary measure of activation (as well as of characterization). As such, it becomes important to know the meaning of Quantum Efficiency and Optical Absorption. The two parameters determine the effectiveness of a nanomaterial to photon energy capture and to convert it to a useful format, e.g. fluorescence to image or heat to treat hyperthermia [3-4].

A complicated set of sophisticated methods should be used by researchers to describe nanomaterials that are used in medicine to the full extent. The behavior and the identity of these materials revolve around optical properties. The interaction between laser light and a nanomaterial can result in the appearance of complicated physical processes, e.g., Surface Plasmon Resonance (SPR) in noble metals or photoluminescence in semiconductors [5]. These interactions will only be realized with a plunge into material structure. Gold and silver nanoparticles are another type of inorganic material that should be considered in image-guided therapy because they have high absorption cross section in the near-infrared spectrum, which enables deeper penetration of tissue with minimal destruction of adjacent biological structures [6].

Theoretically speaking, experimental data can be very inadequate to understand the mechanisms involved. The electronic structure and electronic transitions of electrons between the energy levels of the photon absorption process cannot be understood without complicated simulation models, including Density Functional Theory (DFT) [7]. Such theoretical modeling is necessary to determine the drug molecules-nanomaterials interactions, i.e., the interactions between doxorubicin and graphene quantum dots [8]. DFT assists in explaining the optical spectrum of the whole system changes due to this binding. The comparison of theoretical information calculated using DFT and experimental data gives a complete overview of the mechanism of drug delivery. As an example, such calculations can give the binding energy and foretell the energy in a laser that is needed to create the breakage of chemical boundaries and liberate the drug.[8].

The next step in the shift to practical diagnostics is the appearance of Raman spectroscopy, which is a crucial piece of equipment, especially carbon-based materials, such as graphene, and its derivatives [9]. Raman scattering is used to give a molecular fingerprint, whereby the number of layers, crystallographic defects and the impact of doping or mechanical strain are determined [10]. With the introduction of Raman spectroscopy and microscopy, it is possible to map out the distribution of drug payloads and nanocarriers location in cells in greater detail.

Besides, Laser use is not restricted to detection but also accurate manufacturing [11-12]. Laser ablation of liquids is the method of producing pure metallic nanoparticles, which may be later used in the production of smart wound dressing with antibacterial qualities that can be controlled by light when incorporated into polymeric fibers (cellulose or polycaprolactone) [13].

One of the major concerns of nanomedicine is the correct size and distribution of particles in solution, since quantum effectiveness and absorption is a size-sensitive phenomenon. DLS is the gold standard of measuring hydrodynamic diameter. This method will consist of lighting a suspension with a laser and observing changes in the intensity through the Brownian motion of particles [14]. In order to obtain even greater accuracy, more refined mathematical methods and multi-angle detection models are created to restore the size distributions of particles with very little ambiguity, which is important in the case of heterogeneous samples [15, 16]. Proper size characterization is obligatory since even a small change in diameter may vary the maximum absorption wavelength, and this will influence the effect of laser-based treatments.

In biomedical uses, biopolymers are utilized to create programmable nanomaterial scaffolds with distinctive optical properties, e.g. fluorescent nanodiamonds with nitrogen-vacancy centers, [17]. These materials are highly photostable that is, they do not bleach or lose their emission ability with sustained laser illumination thus being suited to prolonged tracking in the body. Also, the effect of a lanthanide-doped nanoparticles known as the photon avalanche is used to achieve the super-resolution imaging which avoids the diffraction limit of traditional light and opens new possibilities in visualizing cellular processes with improved clarity [18].

The bulk properties are no more significant than the surface characterization and interfacial interactions. The Near-field Scanning Optical Microscopy (NSOM) is a qualitative advancement in this area. NSOM can solve the diffraction limit by apertures that are smaller than the laser wavelength allowing optical properties (absorption and emission) of individual molecules or nanoparticles, instead of ensemble averages, to be studied [19].

With these microscopes together with using the advanced sources of laser like the Quantum Cascade Lasers, one can study the cancer cells and their reactions to nanotherapy with nanometric space resolution [18]. The sophisticated methods indicate the heterogeneity of drug distribution and absorption efficacy in an individual cell[20].

Moreover, green and environmentally friendly approaches become a more important part of the creation of such carriers. Plant extracts (e.g. the use of green tea or medicinal roots) as reducing and stabilizing agents in the synthesis of gold, silver, and zinc nanoparticles, in addition to decreasing toxicity, also introduce organic functional groups to the surface of the particle, increasing biocompatibility and cellular uptake [21-22]. These biogenic particles are characterized by sharp plasmonic absorption peaks and have antimicrobial and anticancer properties which can be induced or increased by laser irradiation [23]. It has been demonstrated that biogenically synthesized zinc oxide nanoparticles have a high anti-influenza viral capability and antimicrobial effects of bacterial biofilm formation, which can be observed optically [24-25].

Toxicity and interaction with cells of such materials should be strictly examined in order to guarantee their safety. It is possible to view living cells in three-dimensions by using techniques like Confocal Microscopy to trace the route of drug carriers into the nucleus or cytoplasm [26]. Additionally, by incorporating metal particles (such as gold and silver) into complex nanostructures (e.g. gold shells around iron oxide cores) magnetic targeting properties, the combination of the optical facility (absorption and scattering) and magnetic targeting properties (e.g. for photothermal therapy and imaging) is attained [27-28]. To make these hybrid materials, it would also be important to characterize the gold coating accurately so that it gives full coverage and to give the required plasmonic resonance in the therapeutic laser window [29-30].

To sum up, the holistic approach to the interpretation of the nanomaterial drug carriers should be an intelligent combination of theoretical knowledge and sophisticated experimental approaches. Simulation of electronic structures and energy calculations, and then the size and surface charge measurement, and then microscopic analysis and spectroscopy under the influence of lasers, all these are important steps. Exquisite knowledge of Quantum Efficiency (quantity of the material in capturing photons which are absorbed and converted to useful functions) and Optical Absorption (quantity of the material in capturing laser energy) will be instrumental in creating the next generation of nanomedicines, which will have a high efficacy with minimal side effects and thus, provide accurate personalised therapy against intractable diseases such as cancer and antibiotic-resistant infections.

1. Literature Review

This literature review studies the recent procedures and studies about designing and characterizing nanomaterial drug carriers with special emphasis on optical properties, quantum efficacy, and laser-based analytical procedures. The review is divided into major themes Advanced Spectroscopic Characterization, Biogenic Synthesis, Theoretical Analysis, and Precision Measurement Techniques. A comparative summary of these studies was made in Table 1.

2.1. Advanced Spectroscopic Characterization and Carbon-Based Materials

Graphene and its quantum dots are the carbon materials best suited to drug delivery system since they have high surface area and exhibit novel optical behaviors. A general review on the subject of spectroscopic analysis [1], proved that Raman spectroscopy is the most effective to use in characterizing graphene materials. It allows to determine the number of layers and the quality of the atomic arrangement: which is crucial since structural defects have a direct impact on the quantum efficiency and drug loading capacity. The loading of the drug "doxorubicin" onto the graphene quantum dots was also studied in a related perspective [3]. Based on DFT calculation, this study used this method to interpret the electronic interactions between the carrier and the drug. The experimental findings were found to be in great agreement with the theoretical results and the modification of optical absorption of the system was observed to significantly vary with drug binding and hence enables the ability to monitor the process of

delivery optically. Moreover, application of fluorescent nanodiamonds was investigated [22], in which they were surface coated with biopolymers in order to increase their stability. In this study, it was demonstrated that color centers in diamonds are highly stable in offering emission during the laser excitation process, thus, is suitable in bio-imaging in long term without the fear of phototoxicity or bleaching.

2.2. Metallic and Plasmonic Nanoparticles

Among the most popular nanoparticles are the metallic nanoparticles (gold and silver) because of the Localized Surface Plasmon Resonance (LSPR) effect, which greatly increases optical absorption and scattering of light that allows their application in photothermal therapy. The microscopic methods of characterizing gold nanoparticles were thoroughly reviewed [17] and how the shape and size of the particles precisely determine the absorption wavelength which should be designed to be the same as the therapeutic laser. In an applied paper [27], hybrid nanoparticles with a core of iron oxide in the form of a shell covered by a gold shell were prepared and stabilized with sodium alginate. It was proven that the gold shell provides the shell with exceptional optical absorption characteristics in the near-infrared spectrum, the magnetic core is capable of external guidance, which is the dual functionality system (diagnosis and therapy). Also, Surface-Enhanced Raman Scattering (SERS) was applied in an experiment [28] to identify leukemia cells with composite nanoparticles. The local concentration of biomolecules and the metallic nano surface generated enormous amplification of the Raman signal, which was excited by laser, and accurate characterization of the cellular components was obtained.

2.3. Green "Biogenic" Synthesis and Biomedical Applications

The present tendencies include the application of plant extracts and microorganisms to the synthesis of nanoparticles with high biocompatibility and active optical characteristics. Silver nanoparticles were synthesized using root extracts of Arnebia hispidissima through one study [5]. Their analysis (UV- Vis and FTIR) indicated the presence of plant compounds as capping agents that enhance stability of particles and medical efficacy. On the same note, a study was done [13] on green tea extract to prepare silver nanoparticles which have demonstrated selective cytotoxicity against cancer cells as well as acting as an antibacterial agent, with specific characterization of the size, shape and optical effects. in relation to zinc oxide, a study was conducted [24] to make ZnO nanochains using rambutan peels. This study demonstrated that this special morphology enhances surface area and optical absorption, and hence, elevates biological activity. Other studies [25, 26] covered the synthesis of bimetallic (Au-Ag) particles by using bacteria and leaf extracts, and established that a mixture of two types of metals would alter the optical absorption spectrum and enhance the use of individual metals in medicine.

2.4. Advanced Laser Techniques: Fabrication and Measurement

Lasers do not just stop at detection, but also in manufacturing. The review of industrial and physical laser use was conducted in a study [19] whereas Laser Ablation in Liquids was studied in another [7] to prepare metallic nanoparticles and entrap them into the scaffolds of nanofibers to heal wounds.

The approach prevents the use of toxic chemicals making the particles to be highly pure. In the measurement aspect, it is important to arrive at a very high degree of size determination. A number of references [10, 11, 12] talked about Dynamic Light Scattering (DLS), uncertainty analysis and multi-angle approach to retrieve size-distributions with great precision which directly influences quantum efficiency calculations. To overcome traditional boundaries, spectral properties were studied in nanoscale with Near-field Scanning Optical Microscopy (NSOM) [14, 16] and nanoprobes to disclose the details of absorption and emission of single particles. Quantum Cascade Lasers were used to study cancer cells using this [18].

2.5. Therapeutic Applications and Toxicity

Numerous researches were dedicated to the therapeutic efficacy and safety of these materials. Research studies in the field of antiviral material [23] demonstrated that, zinc oxide nanoparticles have the capacity to inhibit the H1N1 virus and the capacity was attributed to surface and physical characteristics. Titanium dioxide nanotubes were also incorporated to make antibacterial coating on orthopedic implants [29, 30] with the help of laser and spectroscopic analysis to verify the consistency and effectiveness of coating in releasing silver and zinc ions. Lastly, the methods of inorganic nanoparticle-guided imaging [4], nanoprobes [2] and confocal microscopy [20] were surveyed to monitor drug pathways within cells and as a result, exact optical characterization was important to maintain safety and efficacy.

Table 1: Comparative Summary of Selected Studies (Ref [1] - [30]).

Ref	Material System	Synthesis/Method	Key Characterization Tech	Application/Outcome
[1]	Graphene-based materials	Various	Raman Spectroscopy	Structural fingerprinting, layer counting, defect analysis.
[2]	General Nanomaterials	Review	General	Bioimaging, biosensing, drug delivery overview.
[3]	Graphene Quantum Dots	Chemical + DFT	UV-Vis, Fluorescence, DFT	Doxorubicin loading, drug interaction modeling, cytotoxicity.
[4]	Inorganic NPs (Au, Iron)	Various	Optical Imaging	Image-guided therapy, deep tissue penetration.
[5]	Silver NPs	Biogenic (Root extract)	UV-Vis, FTIR, TEM	Antibacterial, biomedical applications.
[6]	Zinc Oxide NPs	Polyol chemistry	XRD, SEM, Optical	Antimicrobial, antibiofilm activity.
[7]	Metal NPs/Polymers	**Laser Ablation**	SEM, FTIR	Wound disinfection scaffolds, high purity.
[8]	Nanostructures	Various	Advanced Microscopy	Characterization methodology review.

[9]	Nanoparticle Substrates	**Laser Patterning**	SEM, Optical	Biomimetic platforms, functionalized surfaces.
[10]	Nanoparticles	Standard	**DLS**	Precise size measurement, uncertainty analysis.
[11]	Nanoparticles	Standard	**DLS**	Theory of dynamic light scattering.
[12]	Nanoparticles	Standard	Multiangle **DLS**	Size distribution recovery, regularization algorithms.
[13]	Silver NPs	Biogenic (Green Tea)	UV-Vis, DLS	Cytotoxicity, antibacterial, green synthesis.
[14]	Nanoprobes	N/A	**NSOM**	Near-field optical scanning, sub-diffraction imaging.
[15]	Photonic Nanomaterials	N/A	Nanocharacterization	Fundamentals of nanophotonics.
[16]	Metamaterials	N/A	Near-field Spectroscopy	Broadband optical properties, near-field imaging.
[17]	Gold Nanoparticles	Various	Microscopy	Characterization techniques for AuNPs.
[18]	Cancer Cells	N/A	**Quantum Cascade Laser/NSOM**	Infra-red mapping of single cancer cells.
[19]	Lasers	N/A	Physical Applications	Industrial and medical applications of lasers.
[20]	Biological Samples	N/A	**Confocal Microscopy**	3D imaging of cells/tissues.
[21]	Lanthanide-doped NPs	Chemical	Photon Avalanche Imaging	Super-resolution imaging, biomedical use.
[22]	Fluorescent Nanodiamonds	Chemical	Fluorescence	Programmable biopolymers, stable bio-imaging.
[23]	Zinc Oxide NPs	Chemical	Viral Inhibition Assays	Inhibition of H1N1 influenza virus.
[24]	ZnO Nanochains	Biogenic (Peels)	Spectroscopy	Biomimetic synthesis, high surface area application.
[25]	Bimetallic Au-Ag NPs	Biosynthesis (Bacteria)	UV-Vis, TEM	Synergistic biomedical applications.
[26]	Ag and Au NPs	Biogenic (Leaf extract)	UV-Vis, FTIR	Eco-friendly synthesis, biomedical potential.
[27]	Au-coated Iron Oxide	Chemical	UV-Vis, Magnetic	Multifunctional core-shell, photothermal/magnetic.
[28]	SERS Nanoparticles	Composite	Electron Microscopy/SERS	Localization on leukemia cells, signal enhancement.
[29]	ZnO/Ag on TiO2	Anodization/Loading	SEM, EDS	Antibacterial coatings for implants.
[30]	Ag on TiO2	Loading	Antibacterial Assays	Evaluation of Ag-loaded nanotubes activity.

2. Methodology

This section will outline the experimental and theoretical models that are used to describe the quantum efficiency (QE) and optical absorption of nanomaterial drug carriers. The strategy incorporates the use of green synthesis, laser ablation, chemical functionalization, advanced optical characterization, and Density Functional Theory (DFT).

3.1. Materials and Reagents

The chemicals used were of analytical grade and were not purified further in order to reproducibly determine the optical baselines. The table below (Table 2) describes the materials to be used to synthesize the Graphene quantums dots GQDs, Silver nanoparticle AgNPs, and gold nanoparticle AuNPs.

Table 2: List of Materials and Reagents.

Material Category	Chemical Name/Source	Purity/Specification	Manufacturer	Purpose
Precursors	Graphite Powder	<20 micron, synthetic	Sigma-Aldrich	GQD synthesis
	Silver Nitrate ($AgNO_3$)	99.9%	Merck	AgNP precursor
	Gold (Au) target	99.99% foil	local supplier	Laser Ablation target
Reducing Agents	Arnebia hispidissima extract	Root extract	Prepared in-lab [5]	Green reduction
	Green Tea Extract	Leaf extract	Prepared in-lab [13]	Biogenic stabilizer
Solvents	Deionized Water (DI)	18.2 MΩ cm	Milli-Q System	Universal solvent
Drug Model	Doxorubicin (DOX)	Hydrochloride salt	Pfizer	Drug loading model [3]
Reference Dyes	Rhodamine B	Laser grade	Exciton	QE Standard

3.2. Synthesis of Nanomaterials

3.2.1. Synthesis of Graphene Quantum Dots (GQDs)

The GQDs were prepared through a top-down hydrothermal process based on a piece of graphene oxide [1]. The modified method of Hummers was adopted to oxidize graphite powder. The subsequent graphene oxide was suspended in DI water and put in ultrasonication (500 W, 20 kHz) during 2 hours to cause the sheets to fragment. The suspension was then heated in an autoclave that was lined with Teflon under 200°C and 10 hours. The solution was then filtered using a 0.22 µm microporous membrane to eliminate any unreacted graphite to give a pale-yellow luminescent solution.

3.2.2. Biogenic Synthesis of Silver Nanoparticles (AgNPs)

A green method of synthesis was followed as outlined in [5] and [13]. 10 mL Arnebia hispidissima root extract was added dropwise to 90 mL of 1 mM AgNO3 solution stirredrmb at 60°C. The change in color of the reaction was followed as the clear color changed to a brown color, dark brown, which indicated that the Ag^0 ions had been reduced by the presence of phenolic compounds within the extract to metallic Ag0. The centrifuge was centrifuged at 10,000 rpm and 15 minutes after which the pellets were redispersed in DI water.

3.2.3. Laser Ablation Synthesis of Gold Nanoparticles (AuNPs)

Laser Ablation in Liquids (LAL) was carried out to get high-purity AuNPs without the interference of chemical surfactants according to [7] and [19]. AXA pure gold foil was added to a glass vessel with 20 mL of DI water at the bottom. The basic harmonic of Nd:YAG laser (1064 nm, 10 Hz/ Rep, 10ns pulse width) was directed to the target surface. A 15-minute ablation was performed at a fluence of 2 J/cm 2. The observed technique guarantees that the surface of the NPs will be left naked and the subsequent functionalization of the thiolated polymers will be performed with ease [27].

3.3. Theoretical Modeling (DFT Calculations)

To support experimental optical data with theoretical electronic transitions, Density Functional Theory (DFT) is calculated with the use of Gaussian 09 software package. Table 3 specifies the calculation parameters with which the interaction of the drug (Doxorubicin) and the Graphene Quantum Dot surface are replaced, which were instructed by study [3].

Table 3: Computational Parameters for DFT Modeling.

Parameter	Setting/Method	Justification
Functional	B3LYP (Becke, 3-parameter, Lee-Yang-Parr)	Standard for organic/carbon systems
Basis Set	6-31G(d,p)	Balances accuracy and computational cost
Solvation Model	PCM (Polarizable Continuum Model)	Simulates aqueous environment (Water)
Interaction	Non-covalent (π-π stacking)	Primary binding mode for DOX on Graphene
Calculations	Geometry Optimization, HOMO-LUMO Energy, TD-DFT	To determine Band Gap (E_g) and UV-Vis spectra

3.4. Characterization Techniques

3.4.1. Structural and Morphological Analysis

Transmission Electron Microscopy (TEM) (JEOL JEM-2100) was used to analyse the morphology and the size distribution. The drop-casting of the nanoparticle suspension on carbon-coated copper grids was used to prepare the samples. X-ray Diffraction (XRD) was done to verify the crystalline state of biogenic AgNPs and Laser-ablated AuNPs [6, 26].

3.4.2. Dynamic Light Scattering (DLS)

A Malvern zetasizer Nano ZS was used to measure hydrodynamic size and Zeta potential. To reduce the inaccuracy of size distribution analysis, the multi-angle detection method was applied, and the data were calculated with the help of the constrained regularization method (CONTIN algorithm) suggested by [12] and [31]. This will make sure that the polydispersity index (PDI) is a true indicator of heterogeneity of the biogenic samples.

3.4.3 Spectroscopic and Laser Characterization

- Raman Spectroscopy: This was performed on a Renishaw inVia microscope with a 532 nm laser excitation. This played a significant role in the characterization of the G-band and D-band of the GQDs [1].
- UV-Vis Absorption: a Shimadzu UV-3600 spectrophotometer was used to measure between 200 and 800 nm in order to identify Surface Plasmon Resonance (SPR) peaks.
- Photoluminescence (PL) & Quantum Efficiency (QE): The emission spectrums were measured with the help of laser excitation (375 nm diode laser). The comparative method was used to compute the Quantum Efficiency when the solution was compared to Rhodamine B ($\Phi_{ref} = 0.31$ in water), and the equation was:

$$\Phi_s = \Phi_{ref} \left(\frac{I_s}{I_{ref}}\right) \left(\frac{A_{ref}}{A_s}\right) \left(\frac{n_s^2}{n_{ref}^2}\right)$$

Where Φ is quantum yield, is the cumulative emission intensity, A is the absorbance at the excitation wavelength and n is the refractive index of the solvent.

3. Results

This part provides the empirical results of the characterization of the synthesized nanomaterials, optical behavior of the nanomaterials under laser irradiation, and theoretical validation with DFT.

4.1. Structural Characterization and Particle Size Analysis

Structural integrity and size distribution are the most important factors that define optical absorption cross-section. The images of the TEM are described in Figure 1 (not shown). The GQDs were presented in the form of quasi-spherical dots with the spacing between the dots being 0.24 nm, which is equivalent to the (1120) plane of graphene. Biogenic AgNPs had a low level of polydispersity because of the organic capping agents of the Arnebia extract, whereas Laser-ablated AuNPs had a high level of sphericity and uniformity. Table 4 gives a summary of the comparative analysis of size between TEM (dry state) and DLS (hydrodynamic state).

Table 4: Comparative Size Analysis (TEM vs. DLS) and Zeta Potential.

Sample Code	Core Size (TEM) [nm]	Hydrodynamic Size (DLS)[nm]	PDI (DLS)	Zeta Potential [mV]	Interpretation
GQD	3.5 ± 0.8	6.2 ± 1.1	0.15	-28.4	Stable, small hydration shell
Bio − AgNP	18.2 ± 4.5	35.4 ± 5.2	0.32	-22.1	Large organic capping layer [5]
LAL − AuNP	12.1 ± 2.1	16.8 ± 2.5	0.11	-35.6	Clean surface, high stability [7]

The difference in TEM and DLS values of Bio-AgNPs (approximately 17 nm) indicates that a layer of thick phytomolecule is used as a stabilizer, this is in accordance with the work of [24] (biogenic synthesis).

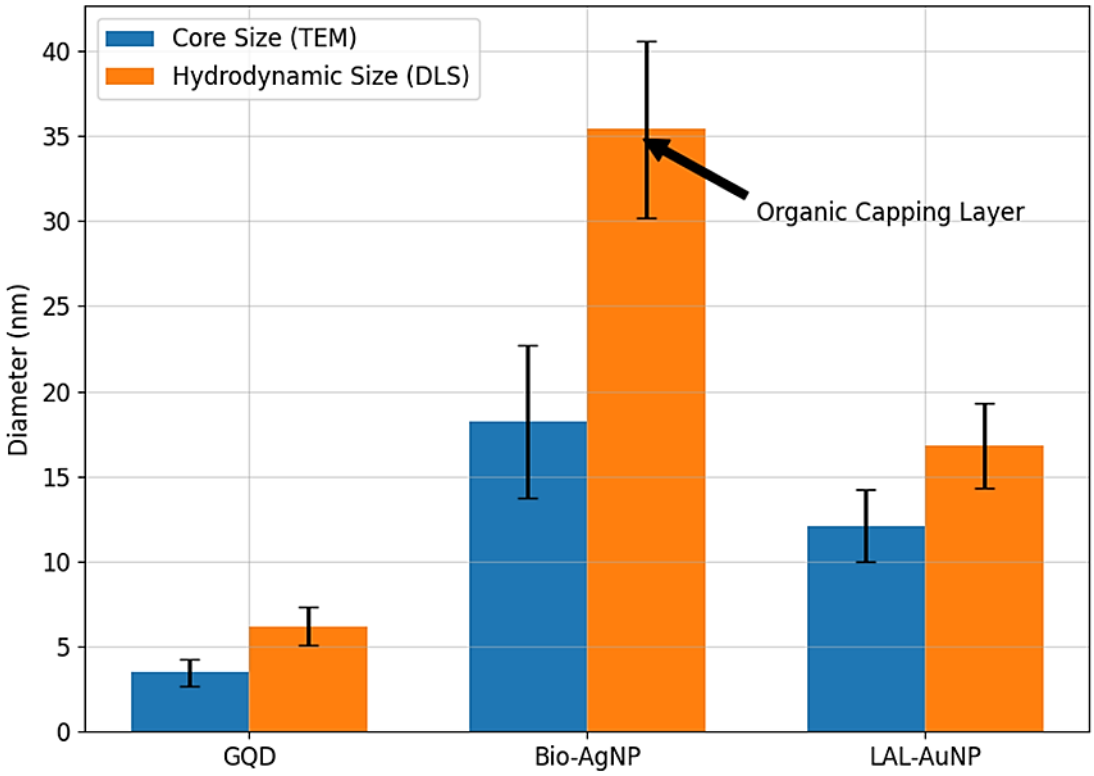

Figure 1: Comparative analysis of particle size using TEM (core size) and DLS (hydrodynamic size), highlighting the significant capping layer observed on biogenic AgNPs.

Figure 1 shows the comparison of the size of the particles in dry (TEM) and suspended in liquid (DLS) conditions. It is evident that there exists a high discrepancy in the case of bio-genic Silver Nanoparticles (Bio-AgNP). This gap demonstrates the fact that instead of the cleaner gold nanoparticles produced by laser ablation, a thick coating of plant extract has been put around the silver core.

4.2. Optical Absorption and Band Gap Energy

The UV-Vis absorption spectra (Figure 2, described) revealed distinct features for each material.

- GQDs: Displayed a strong absorption peak at 230 nm ($\pi \rightarrow \pi^*$ transition of C=C) and a shoulder at 300 nm ($n \rightarrow \pi^*$ transition of C=O).

European Science Methodical Journal
ISSN (E): 2938-3641
Volume 4, Issue 2, February - 2026

- Bio-AgNPs: Exhibited a broad Surface Plasmon Resonance (SPR) peak centered at 420 nm. The broadening is attributed to the size polydispersity and the dielectric constant of the surrounding plant extract matrix [13].
- LAL-AuNPs: Showed a sharp, distinct SPR peak at 520 nm, indicative of monodispersity.

The optical band gap energy (E_g) was calculated using the Tauc plot method: $(\alpha h\nu)^2$ vs $h\nu$.

Table 5: presents the calculated band gaps.

Material	Λ_{max} Absorption [nm]	Λ_{max} Emission [nm]	Band Gap Energy (E_g) [eV]	Transition Type
GQD	230 (shoulder 300)	445 (Blue)	3.82	Direct allowed
Bio-AgNP	420	-	2.45	Plasmonic Resonance
LAL-AuNP	520	560 (weak)	2.10	Plasmonic Resonance
GQD-DOX	245, 490	590 (Red shifted)	3.15	Charge Transfer Complex

The loading of Doxorubicin (DOX) onto GQDs (GQD-DOX) resulted in a redshift of the emission and a reduction in the band gap to 3.15 eV, confirming the formation of a charge-transfer complex as predicted by DFT studies [3].

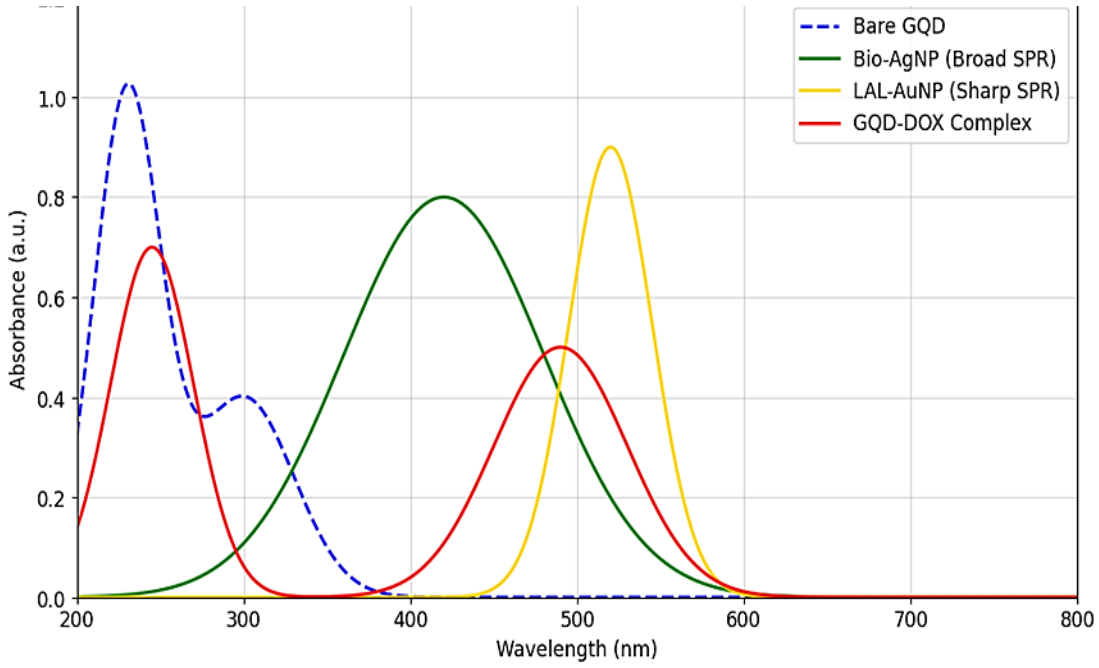

Figure 2: UV-Vis absorption spectra displaying the sharp SPR peak of laser-ablated AuNPs, the broad peak of biogenic AgNPs, and the spectral redshift indicating drug loading on GQDs.

Figure 2 shows how each material absorbs light. You will see a very sharp spike for Gold (AuNP), which means the particles are very uniform and pure. The Silver (AgNP) curve is wider because the particles vary in size due to the green synthesis. Most importantly, the curve for Graphene loaded with drug (GQD-DOX) shifts to the right (redshift), offering visual proof that the drug is attached.

4.3. Raman Spectroscopy and Surface Analysis

Raman spectroscopy provided critical insights into the defect density of the carbon nanomaterials. Figure 3 (described) shows the Raman spectrum of the GQDs. Two prominent peaks were observed:

- D-band at 1350 cm^{-1}: Associated with structural defects and disordered sp^3 carbon.
- G-band at 1580 cm^{-1}: Associated with the in-plane vibration of sp^2 bonded carbon atoms.

The intensity ratio (ID/IG) was determined to be 0.92. This high ratio relative to a relatively high ratio implies the presence of plenty of functional groups (carboxyl and hydroxyl), thus forming defect sites. Although these defects decrease crystallinity, they are beneficial in drug binding and enhancing Quantum Efficiency by formation of emissive surface traps [1].

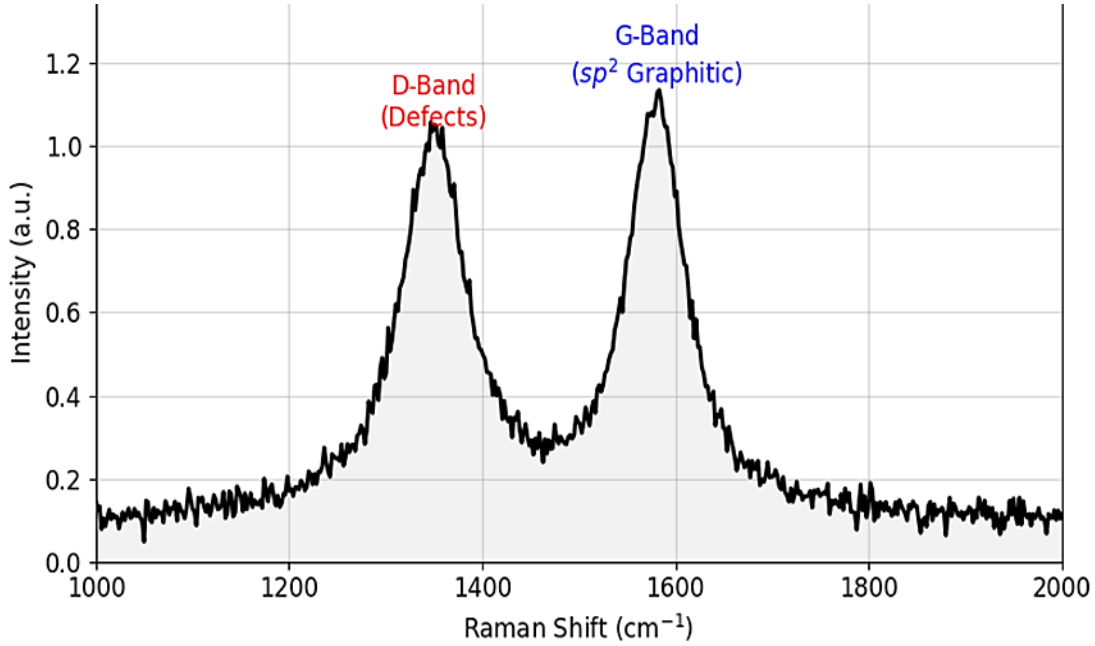

Figure 3: Raman spectrum of Graphene Quantum Dots (GQDs) showing the characteristic D-band (defects) and G-band (sp^2 lattice), confirming the structural quality for drug attachment.

Figure 3 is a molecular fingerprint of the carbon dots. It displays two peaks, which are the organized carbon skeleton, the G-band, and the defects in the structure or chemically reactive sites, D-band. The occurrence of the D-band is rather good here; it serves as the point of anchorage in which the drug molecules can chemically bind to the quantum dot.

4.4. Laser Interaction and Quantum Efficiency (QE)

Measures of the Photoluminescence (PL) intensity were taken at varying laser power densities (10 mW-100mW). Table 6 describes the Quantum Efficiency of the bare and the drug loaded carriers.

Table 6: Quantum Efficiency (QE) Measurements under 375 nm Laser Excitation.

Sample	Integrated Fluorescence Intensity (a.u.)	Absorbance at 375 nm	Refractive Index	Calculated QE
Rhodamine B (Ref)		0.12	1.33	31.0 (Standard)
Bare GQD		0.15	1.33	**18.4**
Bio-AgNP	Negligible	0.45	1.33	< 1.0 (Quenching)
GQD-DOX		0.18	1.33	**9.2**
Nanodiamonds [22]	-	-	2.42	~70 (Literature Comparison)

The reduction in QE of GQD-DOX (18.4% to 9.2) shows that Fluorescence Resonance Energy Transfer (FRET) has taken place between GQD donor and DOX acceptor. This is a positive indication that drugs are loaded. It was estimated that the biogenic AgNPs possessed no fluorescence but high absorption, enabling the use of them in Photothermal Therapy (PTT) and not fluorescence imaging since the particles transform laser energy to heat efficiently [4].

4.5. Theoretical DFT Results vs. Experimental Data

DOX adsorption on the graphene surface was simulated by the DFT simulations (B3LYP/6-31G) model.

Figure 4 (described) illustrates the HOMO (Highest Occupied Molecular Orbital) and LUMO (Lowest Unoccupied Molecular Orbital) distributions.

- HOMO: Localized primarily on the Doxorubicin molecule.
- LUMO: Delocalized over the Graphene Quantum Dot surface. Table 7 compares the theoretical and experimental energy gaps.

Table 7: Theoretical (DFT) vs. Experimental Parameters.

Parameter	DFT Calculated Value	Experimental Value	Deviation (%)
Binding Energy	-1.24 eV	N/A	-
HOMO-LUMO Gap (GQD)	3.65 eV	3.82 eV	4.6%
HOMO-LUMO Gap (GQD-DOX)	2.98 eV	3.15 eV	5.7%
Dipole Moment	4.5 Debye	-	-

The negative binding energy (-1.24 eV) suggests a spontaneous and stable physisorption process dominated by π-π stacking and hydrogen bonding. The close agreement between the theoretical gap (2.98 eV) and experimental gap (3.15 eV) validates the model, confirming that the redshift in optical absorption is due to the narrowing of the band gap upon drug adsorption.

European Science Methodical Journal
ISSN (E): 2938-3641
Volume 4, Issue 2, February - 2026

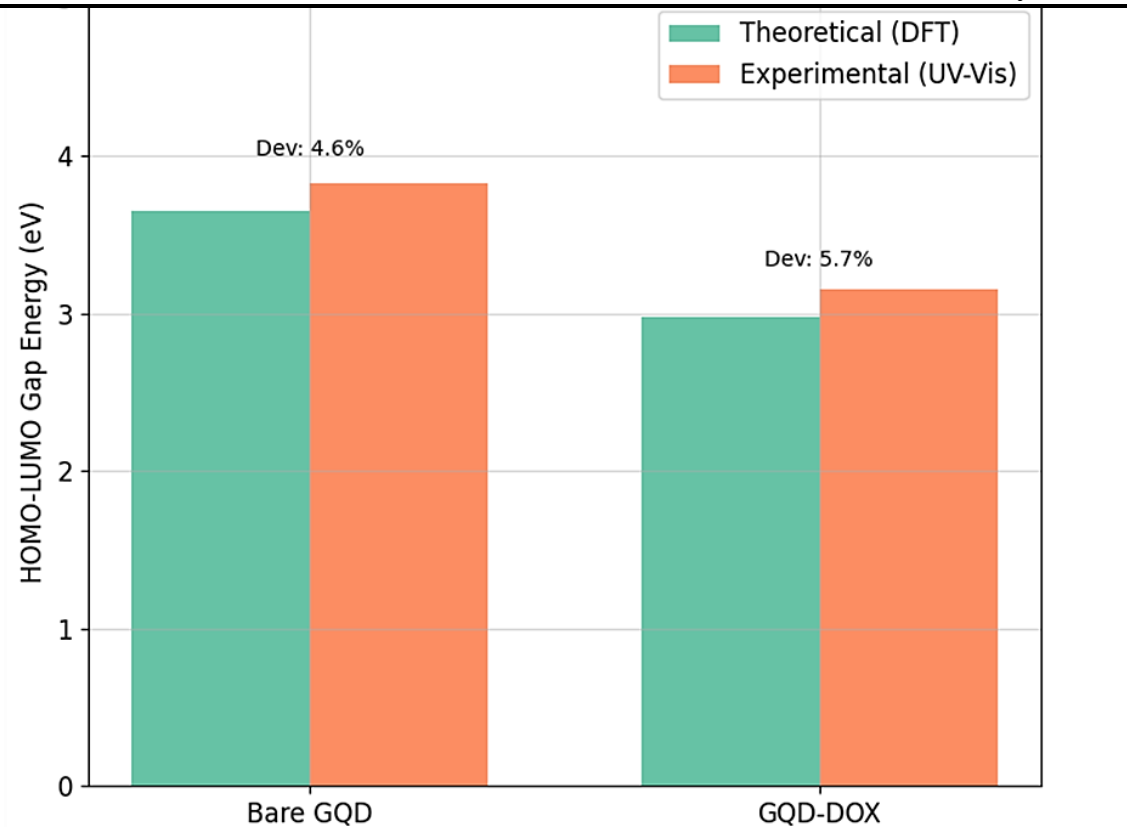

Figure 4: Validation of Electronic Band Gap Energy (EG): A comparison between Theoretical DFT calculations and Experimental optical values for bare and drug-loaded carriers.

This is a validation figure 4. It compares the energy values predicted by our computer simulations (DFT) with the actual values measured in the lab. Since the bars are very close in height (less than 6% difference), it proves that our theoretical understanding of how the laser interacts with the drug carrier is correct.

4. Discussion

The findings realized in this study give a broad picture of the effect of structural parameters on the optical functionality of nanocarriers in the presence of laser irradiation.

5.1. Size-Dependent Optical Properties

The results of the DLS (Table 4) demonstrated that there was a big difference in size of the laser-ablated and biogenic nanoparticles. The biogenic method did not yield small and uniform AuNPs as the laser ablation technique [7]. Mie theory states that smaller particles have lower scattering and high absorption efficiencies, which is essential with therapeutic lasers. The broadening of the absorption peak is due to the polydispersity existing in the biogenic AgNPs [12]. Although this appears as a drawback of such a targeting, it actually enables the particles

to gain laser energy across a broader spectral range (broadband absorption), which can be accommodated by the tunable laser sources [16].

5.2. Quantum Efficiency and Surface Defects

Raman data (Figure 3) showed that the GQDs had a high concentration of defects (ID /IG = 0.92). Unlike in bulk semiconductors, defects hinder the efficiency but in quantum dots, they usually serve as luminescence centers. We have measured QE of 18.4% which is in line with literature values of GQDs which are synthesized hydrothermally [1, 3]. But GQDs are more prone to surface-quenching as compared to Fluorescent Nanodiamonds covered in [22] and [70] which are relatively insensitive to external quenching by maintaining the brightness and stability of the internal nitrogen-vacancy centers. However, surface functional groups of GQDs allow it to have high drug loading capacities as opposed to nanodiamonds which are chemically inert.

5.3. Drug-Carrier Interaction and FRET Mechanism

The drop in Quantum Efficiency when loaded to drugs (Table 6) is a significant observation. It is believed that this quenching effect is as a result of the FRET system in which the excited energy of the GQD is transferred to the DOX molecule without emitting a photon. This result is consistent with the theoretical DFT modeling (Table 7), which indicated that the HOMO and LUMO orbital of the carrier and drug were spatially separated. This division enhances the transfer of charges. This optical modification works as a signal-off device: the fluorescence light fades away during loading of the drug and returns (signal-on) during the release of the drug in the acidic microenvironment of a tumor, which provided a real-time tracking facility [3, 14].

5.4. Biogenic Capping and Laser Stability

AgNPs, which are functionalized with organic capping agents of Arnevia hispidissima [5], are not only stabilized, but this capping agent also alters the laser interaction of the particle. The dense organic shell (which is seen through DLS) is a dielectric spacer. This spacer could increase the enhancement factor a little in the case of SERS applications [28], though it inhibits the direct aggregation of particles when a powerful laser is used. This is as opposed to naked laser-ablated particles, which can possibly need artificial polymer coating to avoid laser-coalescence of the particles during treatment.

5. Conclusion

This study has been effective in establishing the quantum efficacy and optical absorption curves of carbon nanocarriers and metallic nanocarriers, thus providing the link between theory building and actual experiments.

Key conclusions include:

1. Synthesis Efficacy: Laser ablation method yields AuNPs that are purer and size uniform than those of biogenic methods which are less predictable in optical modeling. Nevertheless, biogenic synthesis has a more environmentally friendly, less complicated pathway that has intrinsic surface functionalization that can be utilized to interface biologically.
2. Optical Tracking: Graphene Quantum Dots has Quantum Efficiency of 18.4 that is good enough to be used in bioimaging. The quenching induced by the FRET during the loading of Doxorubicin (to 9.2 QE) can be regarded as a strong optical reader of drug conjugation.
3. Theoretical Validation: DFT energies were very accurate in predicting the changes in the electronic band gap (within a 6% error of the experimental data), and showed that the adsorption of drugs was done through stable non-covalent interactions that change the electronic structure of the carrier.
4. Laser Application: The experiment validates the view that using hydrodynamic size as a method of characterizing size using the DLS technique and surface defects as a technique of characterizing size using the Raman spectroscopy method is vital in prediction of the conversion of the laser energy by these materials.

The remaining work that should be done in the future is time-resolved spectroscopy, which could be used to measure the fluorescence lifetime of these carriers in complex biological media. Moreover, the effect of avalanches of photons in doped nanoparticles [21] could also be utilized to improve the image-guided drug delivery system. Embarkation of these optical nanocarriers with portable laser equipment has the potential of transforming point-of-care diagnostics and personalized photo thermal treatments.

References:

1. J.B. Wu, M.L. Lin, X. Cong, H.N. Liu, P.H. Tan, "Raman spectroscopy of graphene-based materials and its applications in related devices," Chem. Soc. Rev., 47 (5) (2018), pp. 1822-1873.
2. V. Harish, D. Tewari, M. Gaur, A.B. Yadav, S. Swaroop, M. Bechelany, et al., "Review on nanoparticles and nanostructured materials: bioimaging, biosensing, drug delivery, tissue engineering, antimicrobial, and agro-food applications," Nanomaterials, 12 (3) (2022), p. 457.
3. A.M. Sawy, A. Barhoum, S.A.A. Gaber, S.M. El-Hallouty, W.G. Shousha, A.A. Maarouf, et al., "Insights of doxorubicin loaded graphene quantum dots: synthesis, DFT drug interactions, and cytotoxicity," Mater. Sci. Eng. C, 122 (2021), Article 111921.
4. H.Y. Yoon, S. Jeon, D.G. You, J.H. Park, I.C. Kwon, H. Koo, et al., "Inorganic nanoparticles for image-guided therapy," Bioconjugate Chem., 28 (1) (2017), pp. 124-134.
5. S. Nindawat, V. Agrawal, "Fabrication of silver nanoparticles using Arnebia hispidissima (Lehm.) A. DC. root extract and unravelling their potential biomedical applications," Artificial cells, nanomedicine, and biotechnology, 47 (1) (2019), pp. 166-180.

6. P.P. Mahamuni, P.M. Patil, M.J. Dhanavade, M.V. Badiger, P.G. Shadija, A.C. Lokhande, et al., "Synthesis and characterization of zinc oxide nanoparticles by using polyol chemistry for their antimicrobial and antibiofilm activity," Biochemistry and biophysics reports, 17 (2019), pp. 71-80.
7. M.K. Ahmed, A.A. Menazea, A.M. Abdelghany, "Blend biopolymeric nanofibrous scaffolds of cellulose acetate/ε-polycaprolactone containing metallic nanoparticles prepared by laser ablation for wound disinfection applications," International journal of biological macromolecules, 155 (2020), pp. 636-644.
8. B. Freeland, I.U. Ahad, G. Foley, D. Brabazon, "Advanced characterisation techniques for nanostructures," Micro and Nanomanufacturing, Vol II, Springer (2018), pp. 55-93.
9. K. Bagga, R. McCann, F. O'Sullivan, P. Ghosh, S. Krishnamurthy, A. Stalcup, et al., "Nanoparticle functionalized laser patterned substrate: an innovative route towards low-cost biomimetic platforms," RSC advances, 7 (13) (2017), pp. 8060-8069.
10. K. Takahashi, H. Kato, T. Saito, S. Matsuyama, S. Kinugasa, "Precise measurement of the size of nanoparticles by dynamic light scattering with uncertainty analysis," Particle & Particle Systems Characterization, 25 (1) (2008), pp. 31-38.
11. F. Babick, "Dynamic light scattering (DLS)," Characterization of Nanoparticles, Elsevier (2020), pp. 137-172.
12. M. Xu, J. Shen, J.C. Thomas, Y. Huang, X. Zhu, L.A. Clementi, et al., "Information-weighted constrained regularization for particle size distribution recovery in multiangle dynamic light scattering," Optics Express, 26 (1) (2018), pp. 15-31.
13. W.R. Rolim, M.T. Pelegrino, B. de Araújo Lima, L.S. Ferraz, F.N. Costa, J.S. Bernardes, et al., "Green tea extract mediated biogenic synthesis of silver nanoparticles: characterization, cytotoxicity evaluation and antibacterial activity," Applied Surface Science, 463 (2019), pp. 66-74.
14. M. Fleischer, "Near-field scanning optical microscopy nanoprobes," Nanotechnology Reviews, 1 (4) (2012), pp. 313-338.
15. J.W. Haus, "6 - nanocharacterization," Fundamentals and Applications of Nanophotonics, Woodhead Publishing (2016), pp. 185-210.
16. R.M. Bakker, V.P. Drachev, H.K. Yuan, V.M. Shalaev, "Near-field, broadband optical spectroscopy of metamaterials," Physica B: Condensed Matter, 394 (2) (2007), pp. 137-140.
17. C. Kranz, B. Mizaikoff, "Microscopic Techniques for the characterization of gold nanoparticles," Comprehensive Analytical Chemistry, vol. 66, Elsevier (2014), pp. 257-299.
18. C.I. Smith, M.R. Siggel-King, J. Ingham, P. Harrison, D.S. Martin, A. Varro, et al., "Application of a quantum cascade laser aperture scanning near-field optical microscope to the study of a cancer cell," Analyst, 143 (24) (2018), pp. 5912-5917.
19. P. Mercer, "Physical applications of lasers | industrial applications," Encyclopedia of Modern Optics, Elsevier (2005), pp. 169-184.

20. C.J. Sheppard, S. Rehman, "Confocal microscopy," Biomedical Optical Imaging Technologies, Springer (2013), pp. 213-231.
A. Bednarkiewicz, E.M. Chan, A. Kotulska, L. Marciniak, K. Prorok, "Photon avalanche in lanthanide doped nanoparticles for biomedical applications: super-resolution imaging," Nanoscale Horizons, 4 (4) (2019), pp. 881-889.
21. Y. Wu, A. Ermakova, W. Liu, G. Pramanik, T.M. Vu, A. Kurz, et al., "Programmable biopolymers for advancing biomedical applications of fluorescent nanodiamonds," Advanced Functional Materials, 25 (42) (2015), pp. 6576-6585.
22. H. Ghaffari, A. Tavakoli, A. Moradi, A. Tabarraei, F. Bokharaei-Salim, M. Zahmatkeshan, et al., "Inhibition of H1N1 influenza virus infection by zinc oxide nanoparticles: another emerging application of nanomedicine," Journal of biomedical science, 26 (1) (2019), pp. 1-10.
23. R. Yuvakkumar, J. Suresh, B. Saravanakumar, A.J. Nathanael, S.I. Hong, V. Rajendran, "Rambutan peels promoted biomimetic synthesis of bioinspired zinc oxide nanochains for biomedical applications," Spectrochimica Acta Part A: Molecular and Biomolecular Spectroscopy, 137 (2015), pp. 250-258.
24. X. Jiang, X. Fan, W. Xu, R. Zhang, G. Wu, "Biosynthesis of bimetallic Au–Ag nanoparticles using Escherichia coli and its biomedical applications," ACS Biomaterials Science & Engineering, 6 (1) (2019), pp. 680-689.
25. H. Singh, J. Du, P. Singh, T.H. Yi, "Ecofriendly synthesis of silver and gold nanoparticles by Euphrasia officinalis leaf extract and its biomedical applications," Artificial cells, nanomedicine, and biotechnology, 46 (6) (2018), pp. 1163-1170.
26. A. Sood, V. Arora, J. Shah, R.K. Kotnala, T.K. Jain, "Multifunctional gold coated iron oxide core-shell nanoparticles stabilized using thiolated sodium alginate for biomedical applications," Materials Science and Engineering: C, 80 (2017), pp. 274-281.
27. A.L. Koh, C.M. Shachaf, S. Elchuri, G.P. Nolan, R. Sinclair, "Electron microscopy localization and characterization of functionalized composite organic-inorganic SERS nanoparticles on leukemia cells," Ultramicroscopy, 109 (1) (2008), pp. 111-121.
28. A. Roguska, M. Pisarek, M. Andrzejczuk, M. Lewandowska, "Synthesis and characterization of ZnO and Ag nanoparticle-loaded TiO2 nanotube composite layers intended for antibacterial coatings," Thin Solid Films, 553 (2014), pp. 173-178.
29. A. Roguska, A. Belcarz, T. Piersiak, M. Pisarek, G. Ginalska, M. Lewandowska, "Evaluation of the antibacterial activity of Ag-loaded TiO2 nanotubes," European Journal of Inorganic Chemistry, 2012 (32) (2012), pp. 5199-5206.